Available online at www.sciencedirect.com
ScienceDirect
International Journal of Thermal Sciences 46 (2007) 1011–1022
International Journal of Thermal Sciences
www.elsevier.com/locate/ijts

Unsteady forced convection heat/mass transfer around two spheres in tandem at low Reynolds numbers

Gheorghe Juncu *

Politehnica University Bucharest, Catedra Inginerie Chimica, Polizu 1, 78126 Bucharest, Romania

Received 8 August 2006; received in revised form 21 November 2006; accepted 6 December 2006

Available online 5 February 2007

Abstract

This paper presents a computational study of the forced convection heat/mass transfer from two spheres placed in a uniform viscous flow parallel to their line of centers. The temperature/concentration inside the spheres are assumed spatially uniform but not constant in time. Axisymmetric, slow, viscous flow (Stokes flow) around the spheres was considered. The appropriate energy/chemical species balance equations were solved numerically in bispherical coordinates. The finite difference method was used to discretize the mathematical model equations. Various spheres spacing, sizes and physical properties were considered at moderate *Pe* numbers.
© 2007 Elsevier Masson SAS. All rights reserved.

Keywords: Heat/mass transfer; Two spheres; Rigid surface; External flow; Creeping flow

1. Introduction

The importance of the heat/mass transfer from or to a body of spherical shape is reflected by the vast number of works published over the years. Clift et al. [1], Brauer [2], Brounshtein and Shegolev [3], Sadhal et al. [4], Chhabra [5] and Michaelides [6] reviewed the studies published in this field.

In some situations, the single sphere data cannot predict accurately the system behaviour. The interaction between spheres which are moving in close proximity becomes a first interest problem. The heat/mass transfer from two spheres placed in a uniform viscous flow parallel to their line of centers (in tandem) may be considered a first step in the analysis of this interaction.

The heat/mass transfer around two spheres in tandem was analyzed theoretically in:

- [7–11], the stagnant phases case;
- [12], forced convection, creeping flow;
- [13], forced convection, moderate sphere *Re* number;
- [14], combined convection, moderate sphere *Re* number.

Aminzadeh et al. [12] solved the case of two equal size spheres with rigid surface in creeping flow. The Peclet number takes values in the range 0–50. It was found that the overall Sherwood number for either sphere was always less than that of a single isolated sphere. The Navier–Stokes and energy equations have been solved numerically in bispherical coordinates for a pair of equal spheres in tandem at $Re = 40$ and $Pr = 1$ by Tal et al. [13]. Two different spacings were used. As in [12], it is shown that the drag coefficient and the average Nusselt number of either sphere are less than that of a single sphere, the effect being much stronger for the downstream sphere. Chen et al. [14] studied the flow and heat transfer characteristics of laminar combined convection from two isothermal spheres of the same diameter in tandem arrangement. The distance between the spheres centers was constant, being twice the value of the diameter. The values considered for the sphere Reynolds number are in the range 10–100, the fluid phase *Pr* number was assumed equal to 0.7 and the ratio *Gr* (Grashof number for heat transfer)$/Re^2$ varies between 0 and 10. The results presented in [14] are similar to those obtained in [12,13].

The interaction between two spheres was also investigated in thermocapillarity. In almost all articles dedicated to this problem, the effects of the convective transport were neglected and the heat transfer was modeled by the Laplace equation. The ef-

* Tel.: + 40 21 345 0596; fax: + 40 21 345 0596.
E-mail addresses: juncu@easynet.ro, juncugh@netscape.net.

1290-0729/$ – see front matter © 2007 Elsevier Masson SAS. All rights reserved.
doi:10.1016/j.ijthermalsci.2006.12.008

Nomenclature

c	characteristic length, bispherical coordinate system
$\bar{c}$	dimensionless characteristic length, bispherical coordinate system
C_p	heat capacity
d	sphere diameter
k	thermal conductivity
L	distance from the center of the sphere to the origin of the coordinate system
Nu	instantaneous Nusselt number
Pe	fluid phase Peclet number, $Pe = U_\infty d_1 \rho_f C_{p,f}/k_f$
r	radial coordinate in cylindrical coordinate system
t	time
T	temperature
U_∞	free-stream fluid velocity
V	volume
z	axial coordinate in cylindrical coordinate system
Z	dimensionless temperature defined by the relation, $Z_{(s)} = \frac{T_{(s)}-T_\infty}{T_{s,0}-T_\infty}$

Greek letters

η	coordinate in bispherical coordinate system
ξ	coordinate in bispherical coordinate system
Ξ	volume heat capacity ratio, $(\rho_s C_{p,s})/(\rho_f C_{p,f})$
ρ	density
τ	dimensionless time or Fourier number, $\tau = 4tk_f/(\rho_f C_{p,f} d_1^2)$
ψ	stream function
$\bar{\psi}$	dimensionless stream function

Subscripts

f	refers to the fluid phase
s	refers to the spheres
0	initial conditions
1	refers to the upstream sphere
2	refers to the downstream sphere

fects of convective transport were studied only in [15–18]. Different types of approximations (boundary layer, for example) were used in [15–18] to solve the heat/mass balance equations.

The momentum and forced convection heat transfer around three spheres in-line have been investigated numerically in [19] (unconfined spheres) and [20] (the spheres are placed at the axis of a tube). The temperature of the spheres is considered constant. It is shown that for fixed values of the Reynolds and Prandtl numbers, the Nusselt number is maximum for the first sphere and it is reduced progressively for the 2nd and 3rd spheres.

In [7–14] the spheres are considered gradientless, i.e. the concentration/temperature inside the spheres are assumed constant and the shape and volume of the spheres unaffected by the transfer. After Sadhal et al. [4], "physically speaking, a constant condition at the interface implies an infinite heat or mass capacity of the dispersed phase. While the results for transport based on such a constant interface condition give an insight about the resistance of the continuous phase, the validity is in general quite limited. To understand the proper behaviour of a system, full implementation of the interface conditions is needed".

The general formulation of the heat/mass transfer from a body of revolution is that of a conjugate problem. The asymptotic solutions of the conjugate transfer are the *internal* problem [1] and the *external* problem [1]. For the particular situation of heat/mass transfer around two spheres, the influence of spheres interaction on heat/mass transfer rate is expected to be maximum when the transfer is controlled by the fluid, i.e. in the context of the *external* problem. The *external* problem assumes that the sphere is gradientless (the sphere has *uniform properties*). The condition of *uniform sphere properties* is fulfilled if the relaxation time inside the sphere is considerably smaller than the relaxation time in the fluid. The transfer is hundreds of times (at least) faster inside the spheres than in the fluid. In terms of physical quantities, this condition means values considerably greater than one for the conductivity ratio or the quantity (diffusivity ratio) × (Henry number). Note that these ratios are defined as (sphere's property)/(environmental fluid property).

The aim of this work is to extend the analysis from [12–14] to the spheres with spatially uniform, but changing with time, concentration/temperature. The surfaces of the spheres were considered rigid. Stokes flow around the spheres was assumed. At moderate values of the Pe number, i.e. $Pe = 100$, the influence of the physical properties ratio on the heat/mass transfer rate was analyzed for spheres of equal/different diameters and identical/different physical properties. Different spheres spacing was considered.

2. Basic equations

Consider the steady, axisymmetric, creeping flow of a Newtonian incompressible fluid past two spheres of diameter d_1 and d_2, respectively, parallel to their line of centers as shown in Fig. 1. We assume that the diameters of the spheres are considerably higher than the molecular mean free path of the surrounding fluid. Oscillations and rotation of the spheres do not occur during the movement. The spheres have the same initial concentration/temperature. Due to the complexity of the problem, the following supplementary assumptions are considered:

(i) during the heat/mass transfer, the volume and the shape of the sphere remain constant;
(ii) the concentration/temperature inside the spheres is spatially uniform but not constant in time;
(iii) the physical properties are constant;
(iv) during the heat/mass transfer, the distance between the spheres remains constant;

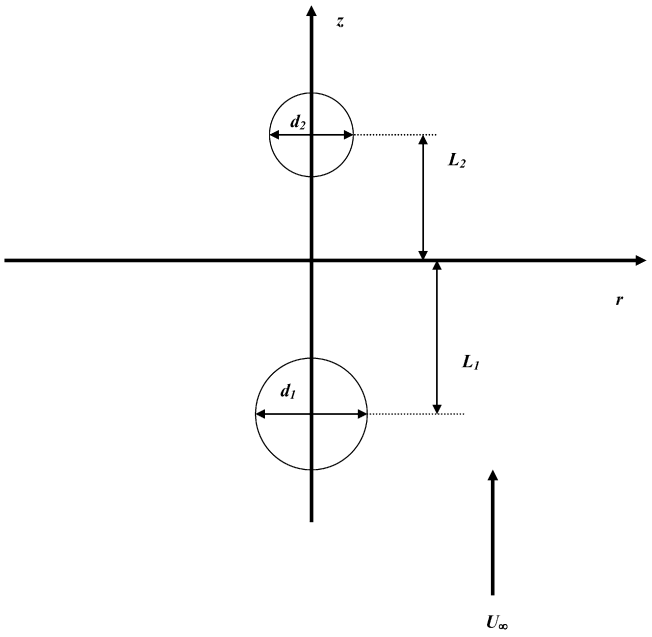

Fig. 1. Schematic of the problem.

(v) no phase change occurs during the heat/mass transfer;
(vi) no chemical reaction inside the spheres or in the surrounding fluid;
(vii) the effects of free convection, viscous dissipation and radiation are negligible;
(viii) in the case of mass transfer, the only diffusion mechanism is the Fick diffusion mechanism;
(ix) at the interface, thermodynamic equilibrium is established instantaneously.

The assumption (iv) needs supplementary discussions. Considering the spheres freely suspended in the surrounding flowing fluid, the assumption (iv) is satisfied if the net force (the resultant of the forces) acting on each sphere vanishes. The forces usually taken into consideration are: the buoyancy force, F_b, the gravity force, F_g, and the hydrodynamic interaction force, F_h. For spheres with identical physical properties and equal diameters in Stokes flow, the relation $F_g - F_b - F_h = 0$ can be satisfied in normal conditions. The situation is more complex for spheres with different physical properties and/or different diameters. For some parameter values used in this work, the assumption (iv) is fulfilled if the spheres are immobilized by mechanical devices or if other forces act on the system.

The assumptions practiced in this work are those usually employed in the analysis of the analogy between heat and mass transfer. For the simplicity and clarity of the presentation, in the remainder of this work, we will use only the terminology specific to heat transfer. This does not mean however that the implication of the present results in mass transfer should be ignored.

Under the previous assumptions, for spheres with spatially uniform temperature, the heat balance equations for an axisymmetrical flow field in general orthogonal curvilinear coordinates α, β, ϕ (axisymmetric versus the coordinate ϕ) are:

- fluid phase:

$$\rho_f C_{p,f}\left(\frac{\partial T_f}{\partial t} + v_\alpha \frac{1}{h_\alpha}\frac{\partial T_f}{\partial \alpha} + v_\beta \frac{1}{h_\beta}\frac{\partial T_f}{\partial \beta}\right) = k_f \frac{1}{h_\alpha h_\beta h_\phi}\left[\frac{\partial}{\partial \alpha}\left(\frac{h_\beta h_\phi}{h_\alpha}\frac{\partial T_f}{\partial \alpha}\right) + \frac{\partial}{\partial \beta}\left(\frac{h_\alpha h_\phi}{h_\beta}\frac{\partial T_f}{\partial \beta}\right)\right] \tag{1a}$$

- sphere:

$$\rho_{s,i} C_{p,s,i} V_{s,i} \frac{\partial T_s}{\partial t} = k_f \iint_{\sigma_i} \frac{1}{h_\alpha}\frac{\partial T_f}{\partial \alpha} h_\beta h_\phi \, d\beta \, d\phi \quad i = 1, 2 \tag{1b}$$

where

$$v_\alpha = -\frac{1}{h_\beta h_\phi}\frac{\partial \psi}{\partial \beta}, \qquad v_\beta = \frac{1}{h_\alpha h_\phi}\frac{\partial \psi}{\partial \alpha}$$

ψ is the stream-function and σ_i the spheres surfaces.

It is convenient to use the bispherical coordinate system [21–23] to solve numerically this problem. Let a system of axisymmetric cylindrical coordinates (r, z) be chosen so that the centres of the spheres lie along the z-axis (see Fig. 1). The axisymmetric bispherical coordinate system (ξ, η) and the axisymmetric cylindrical coordinates (r, z) are related via the transformation laws:

$$r = \frac{c \sin \xi}{\cosh \eta - \cos \xi}; \qquad z = \frac{c \sinh \eta}{\cosh \eta - \cos \xi}$$

where $c > 0$ is a characteristic length. This transformation maps the right half of the rz-plane (from which the surface occupied by the spheres is excluded) into the rectangle $\eta_1 \leqslant \eta \leqslant \eta_2$, $0 \leqslant \xi \leqslant \pi$ ($\eta_1 < 0$, $\eta_2 > 0$). The surfaces of the spheres are located at $\eta = \eta_1$ and $\eta = \eta_2$. The relations between η_1, η_2, the diameters of the spheres, d_1, d_2, and the distances, L_1, L_2, of their centers from the origin of the coordinates system are:

$$\frac{d_i}{2} = \frac{c}{\sinh |\eta_i|}; \quad L_i = c \coth |\eta_i|, \quad i = 1, 2 \tag{2}$$

The scale factors (metric coefficients) $h_\alpha, h_\beta, h_\phi$, for the bispherical coordinate system are:

$$h_\alpha = h_\eta = \frac{c}{\cosh \eta - \cos \xi}$$

$$h_\beta = h_\xi = \frac{c}{\cosh \eta - \cos \xi}$$

$$h_\phi = \frac{c \sin \xi}{\cosh \eta - \cos \xi}$$

We define the following dimensionless variables and groups (the radius of the upstream sphere is considered as the length scale and the free stream velocity U_∞ as the velocity scale)

$$\bar{c} = \frac{2c}{d_1}, \qquad Z_{(s)} = \frac{T_{(s)} - T_\infty}{T_{s,0} - T_\infty}$$

$$\tau = \frac{4 t k_f}{\rho_f C_{p,f} d_1^2}, \qquad \bar{\psi} = \frac{4\psi}{U_\infty d_1^2}$$

$$Pe = \frac{\rho_f C_{p,f} U_\infty d_1}{k_f}, \qquad \Xi = \frac{\rho_s C_{p,s}}{\rho_f C_{p,f}}$$

After η and ξ are substituted for α and β in (1), the non-dimensional conservation balances equations for the thermal energy in axisymmetric bispherical coordinates are:

$$\frac{\partial Z}{\partial \tau}+\frac{Pe}{2}\frac{A^3}{\sin\xi}\left(\frac{\partial \bar{\psi}}{\partial \xi}\frac{\partial Z}{\partial \eta}-\frac{\partial \bar{\psi}}{\partial \eta}\frac{\partial Z}{\partial \xi}\right) = A^2\left(\frac{\partial^2 Z}{\partial \eta^2}+\frac{\partial^2 Z}{\partial \xi^2}\right)-\frac{A\sinh\eta}{\bar{c}}\frac{\partial Z}{\partial \eta} + \frac{A(\cosh\eta\cos\xi-1)}{\bar{c}\sin\xi}\frac{\partial Z}{\partial \xi} \tag{3a}$$

$$\left(\frac{d_i}{d_1}\right)^3\frac{dZ_{s,i}}{d\tau} = \pm\frac{3}{2}\Xi_i^{-1}\int_0^{\pi}\left.\frac{\partial Z}{\partial \eta}\right|_{\eta=\eta_i}\frac{\bar{c}\sin\xi}{\cosh\eta_i-\cos\xi}\,d\xi, \quad i=1,2 \tag{3b}$$

where

$$A=\frac{\cosh\eta-\cos\xi}{\bar{c}}$$

The appropriate boundary conditions are:

- spheres surfaces ($\eta=\eta_i$, $i=1,2$)

$$Z=Z_{s,i}, \quad i=1,2 \tag{4a}$$

- free stream ($\eta=\xi=0$)

$$Z=0 \tag{4b}$$

- symmetry axis ($\xi=0$ and $\eta\neq 0$, $\xi=\pi$)

$$\frac{\partial Z}{\partial \xi}=0 \tag{4c}$$

The dimensionless initial conditions are:

$$\tau=0, \quad Z_{si}=1, \quad Z(\eta\neq\eta_i)=0, \quad i=1,2 \tag{5}$$

The quantities of interest used to characterize the heat transfer are:

- spheres dimensionless temperature, $Z_{s,1}$ and $Z_{s,2}$;
- instantaneous local Nusselt number, $Nu_i(\xi)$, $i=1,2$;
- overall (surface average) instantaneous Nusselt number, Nu_i, $i=1,2$.

Considering as driving force the instantaneous temperature difference ($T_{s,i}-T_\infty$) and the diameters of the spheres as characteristic length, $Nu_i(\xi)$ and Nu_i were calculated in bispherical coordinates by the relations:

$$Nu_i(\xi)=\mp\frac{d_i}{d_1}\frac{2}{Z_{s,i}}\frac{\cosh\eta_i-\cos\xi}{\bar{c}}\left.\frac{\partial Z}{\partial \eta}\right|_{\eta=\eta_i}, \quad i=1,2 \tag{6a}$$

$$Nu_i=\mp\frac{d_i}{d_1}Z_{s,i}^{-1}\frac{\sinh^2\eta_i}{\bar{c}}\int_0^{\pi}\left.\frac{\partial Z}{\partial \eta}\right|_{\eta=\eta_i}\frac{\sin\xi}{\cosh\eta_i-\cos\xi}\,d\xi \quad i=1,2 \tag{6b}$$

The present relations used to calculate the *Nu* numbers do not follow the classical relations presented in [2] (the initial temperature difference is used as driving force in [2]). The *Nu* number based on the initial temperature difference represents the instantaneous average dimensionless heat flux on the surface of the spheres. In all situations, this *Nu* number decreases monotonously in time and tends asymptotically to zero (the asymptotic value corresponds to the end of the process). In heat/mass transfer computations its time average value is usually related to the difference between the temperature of the spheres and the environmental fluid.

The present *Nu* number is not a direct measure of the intensity of the process, but it has a nonzero asymptotic limit. This asymptotic value is reached when the dimensionless temperature of the spheres and the dimensionless temperature gradient on the surface of the spheres obey the same exponential decrease in time. However, the technical relevance of this asymptotic value depends on the temperature value at which it is attained. In heat/mass transfer computations its time average value is usually used in connection with the logarithmic mean difference between the temperature of the spheres and the environmental fluid.

3. Method of solution

The values of the dimensionless stream-function were calculated numerically. The numerical solving of the fourth-order stream-function equation in bispherical coordinates is presented in [24].

The energy balance equations were solved numerically. The mathematical model equations (3) is a system formed by a 2D linear parabolic partial differential equation (PDE) that describes the heat transfer in the fluid phase and two linear ordinary differential equation (ODE) that describes the energy balance of the spheres. The 2D domain $[\eta_1,\eta_2]\times[0,\pi]$ was transformed into the unit square. Eq. (3a) was discretized with the exponentially fitted scheme [25], on uniform grids with $N\times N$ points, $N=65, 129, 257$ and 513. The mesh step size h is equal to $h=1/(N-1)$. Let us consider that the numerical values of the dimensionless temperature at time τ are known. The values at the time $\tau+\Delta\tau$ were calculated as follows:

- the values on the spheres surfaces were calculated by integrating (3b) from τ to $\tau+\Delta\tau$ with an explicit modified Euler algorithm; the integral from relations (3b) was calculated by the Simpson 3/8 rule using the local heat flux values available at time τ;
- the values of the dimensionless temperature in the fluid phase were calculated by the implicit ADI method using the spheres surfaces values computed in the previous step as boundary conditions (relations (4a)).

The time step was variable and changed from the start of the computation to the final stage. The initial and final values of the time step depend on the parameter values.

For the spheres with constant temperature, we can analyze the accuracy and the grid dependence of the numerical solutions using the steady values of the average *Nu* numbers. A sample from our numerical experiments is presented in Table 1. Table 1 shows that starting from the grid with $N=129$, the relative er-

Table 1
Mesh behaviour of the solution for equal size spheres with constant temperature

Nu	$2L/d$	Mesh			
		65×65	129×129	257×257	513×513
Nu_1	1.25	4.9519	4.9797	4.9895	4.9927
Nu_2		3.3757	3.4328	3.4491	3.4537
Nu_1	2	5.1747	5.1815	5.1847	5.1863
Nu_2		3.7919	3.8299	3.8406	3.8436
Nu_1	3	5.2688	5.2917	5.2948	5.2954
Nu_2		4.0837	4.1257	4.1380	4.1417

rors in the average Nu numbers are smaller than 1% and the numerical solution computed on the mesh with $N = 513$ can be considered grid independent. For the spheres with spatially uniform temperature the time evolution of Nu_i and $Z_{s,i}$ were analyzed for different N and integration time steps values. Also, the discrete Euclidean norm of the residuals was monitored. The values selected for N and the time integration steps correspond to a grid and time step independent solution (the relative errors in Nu_i and $Z_{s,i}$ are smaller than 1%).

4. Results

Three problems are analyzed in this section. First, the influence of the spheres spacing on the heat transfer rate is analyzed for two spheres with identical physical properties, i.e. $\Xi_1 = \Xi_2 = \Xi$, and equal diameters. The second refers to the spheres with different physical properties and the same diameter. The heat transfer interaction from spheres with different diameters is the third problem studied. Each problem is presented in a distinct sub-section. In all computations, the volume heat capacity ratio, Ξ, takes values from 0.01 to 100 and the Peclet number based on the upstream sphere diameter, Pe, is considered equal to 100. For metallic spheres, porous or smooth, Ξ takes values considerably greater than one, if the environmental medium is a gas, and in the range (0.1, 10), if the environmental medium is liquid. For a mass transfer process, Ξ is the Henry number. Taking into consideration the fact that in the presence of the contaminants, a fluid sphere behaves as a rigid sphere, Ξ can take values considerably smaller than one. The results presented were obtained on a 513×513 mesh points.

4.1. Spheres of equal sizes and identical physical properties

If $d_1 = d_2 = d$, it results from relations (2) that $-\eta_1 = \eta_2$ and $L_1 = L_2 = L$. The values selected for L are: $L = 1.25d, 2d, 3d$. These values correspond to a gap between spheres equal to $0.25d$, d and $2d$, respectively.

In the case of Stokes flow around two equal-sized spheres in tandem, the spheres have identical values of the drag coefficient [22,26], surface pressure, vorticity, and so on. The stream-function is symmetric about the r-axis. The hydrodynamic environment around each sphere is the same. Under these conditions, for this case, the results obtained for the heat transfer may be viewed as the image of a pure thermal interaction.

Table 2
Average Nu numbers for spheres in tandem with constant temperature

d_1/d_2	$2L_1/d_1$	Nu_1	Nu_2	Nu_{iso}	Nu_1/Nu_{iso}	Nu_2/Nu_{iso}
1	1.25	4.99	3.454	5.611	0.889	0.616
1	2	5.186	3.844		0.924	0.685
1	3	5.295	4.142		0.944	0.738
0.5	1.25	4.276	5.372		0.762	0.791[a]
0.5	2	4.724	5.436		0.842	0.801[a]
2	1.25	5.369	2.183		0.957	0.466[b]
2	2	5.41	2.821		0.964	0.602[b]

[a] $Nu_{\text{iso}} = 6.79$ (for $Pe = 200$).
[b] $Nu_{\text{iso}} = 4.684$ (for $Pe = 50$).

The first task in any numerical work is to reproduce published results accurately. Unfortunately, there are no data in literature to verify the accuracy of the present computations. The simulation of the case of spheres with constant temperature can be viewed as a partial validation of the present computation. Even for the case of constant sphere's temperature, Aminzadeh et al. [12] presented numerical values of the average Sherwood number only for $Pe = 0$, while the results from [13,14] were obtained in a different hydrodynamic regime.

The values of the average Nu number computed in this work for $\Xi^{-1} = 0$, i.e. spheres with constant temperature, are given in Table 2. Table 2 shows that the present values of the reduction factor (the reduction factor is the ratio between the average Nu number for spheres in tandem and the average Nu number for an isolated sphere) for the leading sphere are comparable with those obtained in [13]. For the downstream sphere, the values of the reduction factor presented in [13] are smaller than the present ones. Note that the comparison between the present work and [13] can be only guiding, due to the different hydrodynamic regimes.

The case of two equal size spheres separated by sufficiently large distance so that each sphere behaves like an isolated one, may be used as accuracy test. For the present situation, i.e. creeping flow and $Pe = 100$, the relative difference between Nu_1 and the Nu value calculated for an isolated sphere, Nu_{iso}, becomes smaller than 1% for $2L/d \geqslant 21$. The convergence of Nu_2 to Nu_{iso} is slower. For example, $Nu_2/Nu_{\text{iso}} = 0.9295$ for $2L/d = 21$, $Nu_2/Nu_{\text{iso}} = 0.966$ for $2L/d = 51$ and $Nu_2/Nu_{\text{iso}} = 0.981$ for $2L/d = 101$. Note that even for the analytical solution of Stimson and Jeffery, the correction factor tends asymptotically to 1 (it is equal to 1 for an infinite distance between spheres).

The time variation of the average Nu numbers is plotted in Figs. 2 for different values of the heat capacity ratio. For each Ξ value, the isolated (single) sphere results are also depicted. The isolated sphere data were plotted as comparison criterion for the asymptotic values. The case of the spheres with constant temperatures is presented in Fig. 2(a). Fig. 3 shows the time variation of the dimensionless temperature of the spheres for $\Xi = 100$ (Fig. 3(a)) and $\Xi = 1$ (Fig. 3(b)). The connections between Nu_i and Z_i are obvious.

Figs. 2(b)–2(d) show that the average Nu numbers for spheres with uniform temperature exhibit a different time evolution in comparison with spheres with constant temperature.

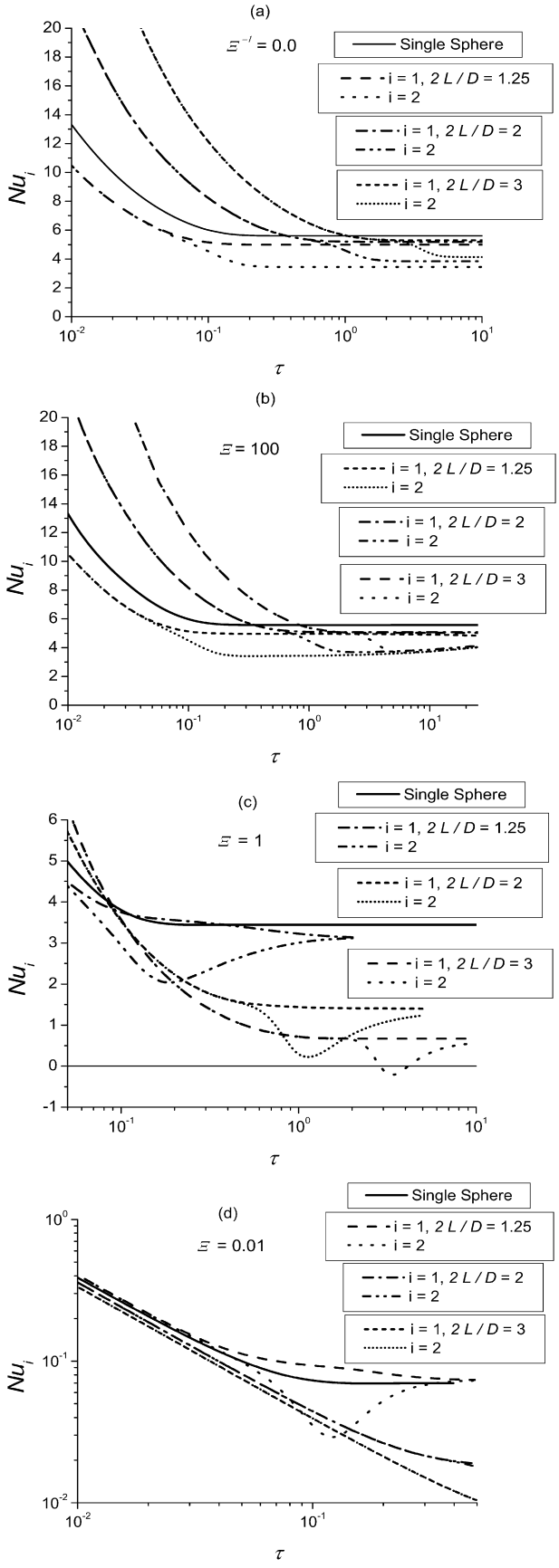

Fig. 2. Time evolution of the average *Nu* numbers for different spheres spacing and different values of the volume heat capacity ratio; (a) spheres with constant temperature; (b) $\Xi = 100$; (c) $\Xi = 1$; (d) $\Xi = 0.01$.

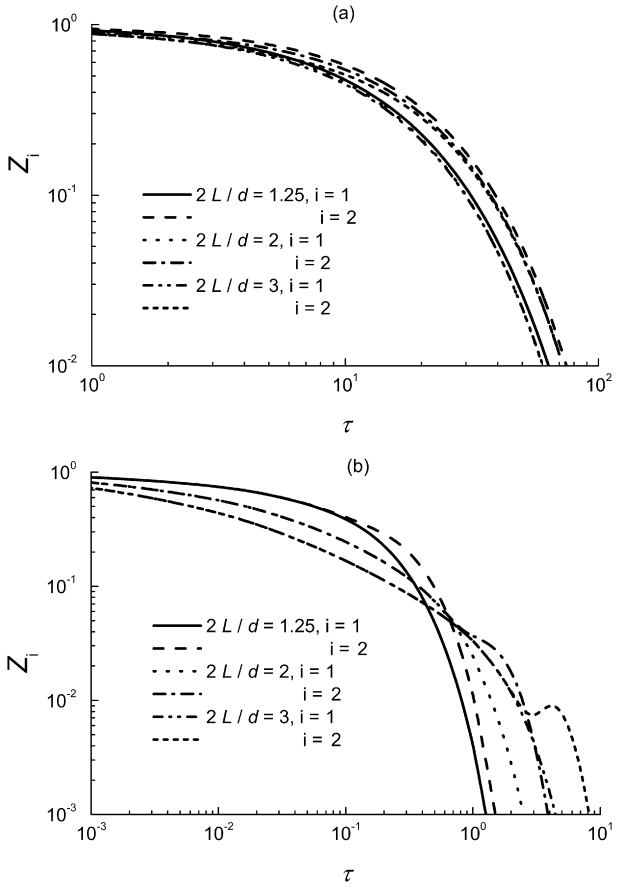

Fig. 3. Time variation of the dimensionless temperature of the spheres for different spheres spacing and different values of the volume heat capacity ratio; (a) $\Xi = 100$; (b) $\Xi = 1$.

The main facts are (the results obtained for $0.1 \leqslant \Xi \leqslant 10$ are similar to those presented in Fig. 2(c)):

- The *Nu* number of the trailing sphere, Nu_2, does not tend asymptotically to a value different from Nu_1. For $\tau \to \infty$, both *Nu* numbers tend to the same value.
- The increase in $2L/d$ increases the asymptotic *Nu* values only for $\Xi = 100$ and $2L/d$ in the range 1.25–2. In all the other cases the increase in $2L/d$ from 1.25 to 3 decreases the asymptotic *Nu* values.
- Negative values of Nu_2 occur for $\Xi = 1, 2L/d = 3$ and $\Xi = 0.1, 2L/d = 2$ and 3.
- For $\Xi = 0.1$ and 0.01 and $2L/d = 1.25$, the asymptotic *Nu* values of the tandem spheres tend to a value greater than the asymptotic *Nu* value of the isolated sphere.

For $\Xi = 0.01$ and $2L/d = 2; 3$, Nu_1 and Nu_2 separate when $Z_i \approx 10^{-4}$. The split in the time evolution of the two *Nu* numbers does not appear very clearly in Fig. 2(d) because we stopped the time integration when $Z_i \leqslant 10^{-4}$.

To unravel the rules of the present interaction we plotted in Fig. 4 (for $2L/d = 1.25$) and Fig. 5 (for $2L/d = 2$) the dimensionless temperature profiles in the interaction zone, i.e. $\pi/2 \leqslant \xi \leqslant \pi$. The corresponding values of the local *Nu* numbers are presented in Figs. 6 and 7, respectively. Two cases are

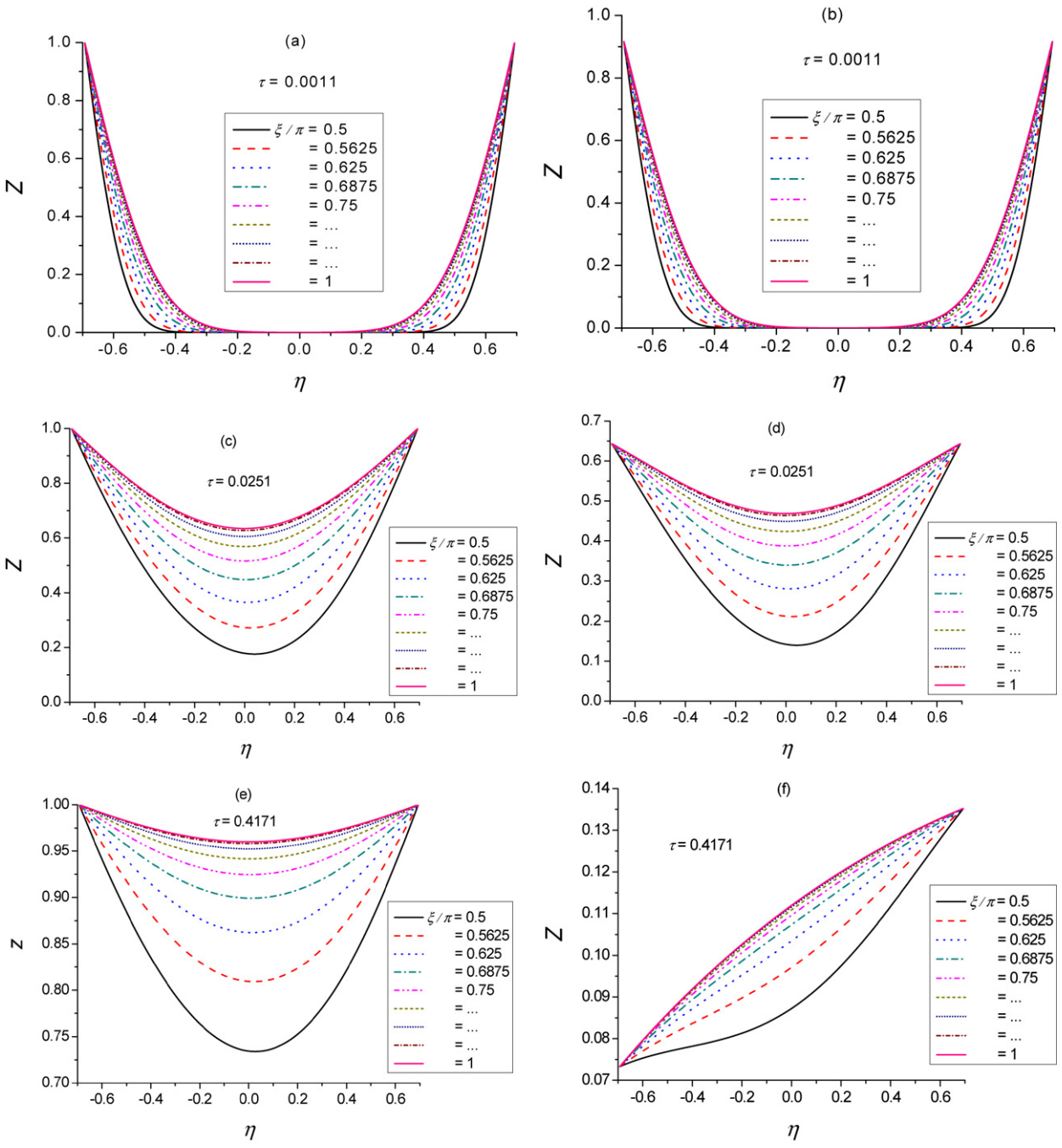

Fig. 4. Dimensionless temperature profiles in the interaction zone for $2L/d = 1.25$; (a), (c), (e) spheres with constant temperature; (b), (d), (f) spheres with uniform temperature.

presented in parallel: the spheres with constant temperature and the spheres with uniform temperature for $\Xi = 1$.

The dimensionless temperature profiles in the interaction zone at short times, when the conduction is the dominant mechanism of transport and there is no interaction, can be viewed in Figs. 4(a), (b) and 5(a), (b). Figs. 4(c), (d) and 5(c), (d) show the dimensionless temperature profiles when the two *Nu* numbers separates. The behaviour of the systems after the *Nu* numbers separation is depicted in Figs. 4(f) and 5(f). The steady state dimensionless temperature profiles for the spheres with constant temperature are plotted in Figs. 4(e) and 5(e). Note that in Figs. 6 and 7, for the upstream sphere the front stagnation point is located at $\xi/\pi = 0$ while the rear stagnation point at $\xi/\pi = 1$. For the downstream sphere, the front stagnation point is located at $\xi/\pi = 1$ while the rear stagnation point at $\xi/\pi = 0$. In Fig. 7(b) the values of the local *Nu* number calculated for $\tau = 0.0011$ are not plotted in order to avoid a strong compression of the other data. The values of the local *Nu* numbers for the spheres with uniform temperature at $\Xi = 1, 2L/d = 2$ and $\tau = 0.0011$ are practically equal with those plotted in Fig. 7(a).

Let us consider two elements of fluid that meet on a streamline in the vicinity of the downstream sphere. One of these ele-

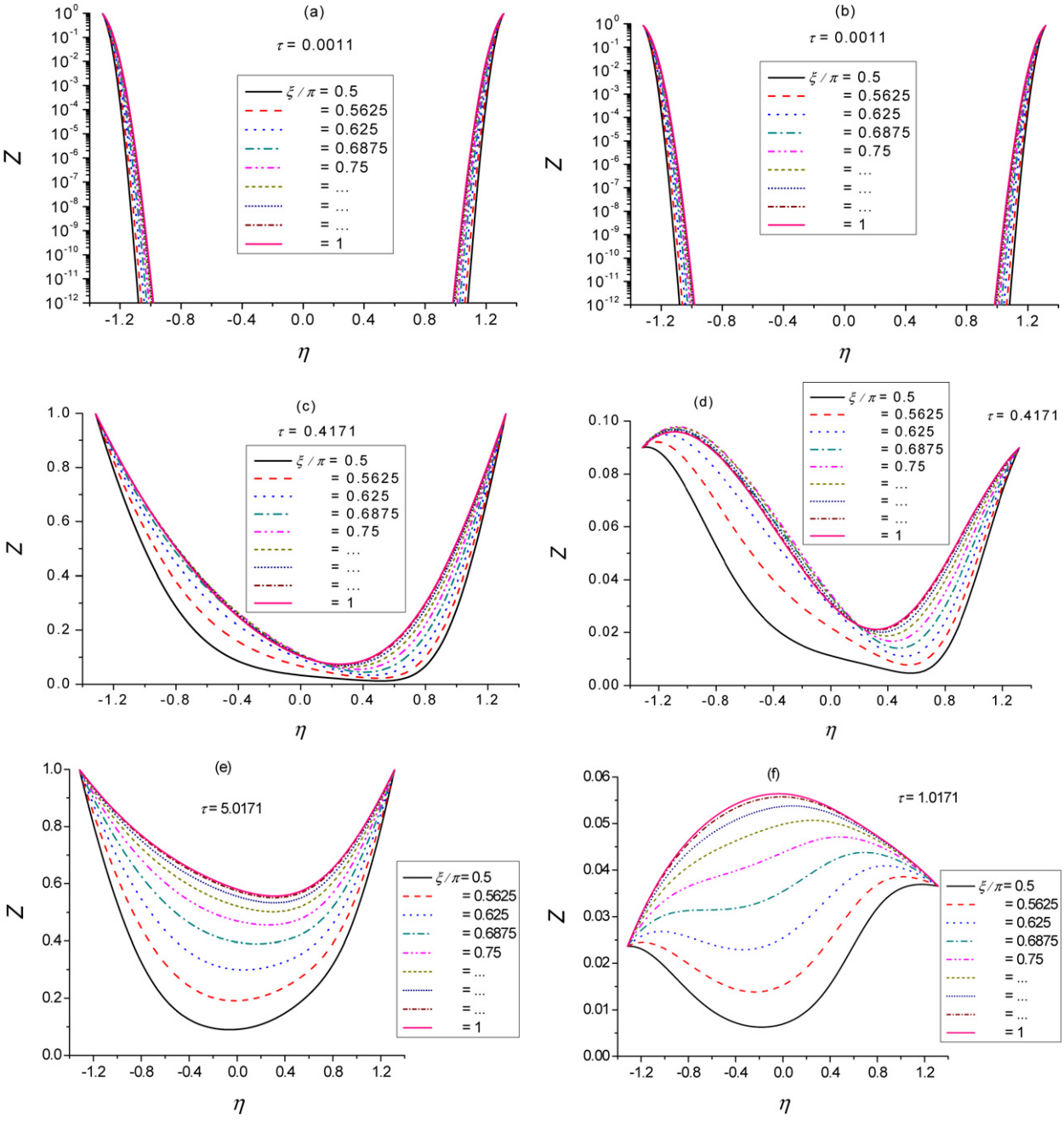

Fig. 5. Dimensionless temperature profiles in the interaction zone for $2L/d = 2$; (a), (c), (e) spheres with constant temperature; (b), (d), (f) spheres with uniform temperature.

ments is coming from the upstream sphere with the dimensionless temperature Z'. The other element has the dimensionless temperature Z'', due to the heat transfer from the downstream sphere. The meeting of the two elements leads to a *blocking* in the heat transfer rate for both spheres. In the early stages of the interaction, we may assume that $Z' < Z''$. In this case both spheres behave as a single object, with the same average heat transfer rate. In time Z' increases. When $Z' \approx Z''$, the *pressure* exerted by the upstream sphere increases considerably and the heat transfer rate of the downstream sphere decreases. At this moment, the time variation of the two *Nu* numbers separates. Thus we may consider that two stages of interaction exist. Also, from Fig. 2, an important observation that should be drawn is: Nu_1 does not vary significantly after the separation point; the asymptotic values of Nu_1 and Nu_1 values at the separation moment are approximately the same.

The scenario described previously applies to both systems presented in Figs. 4–7, i.e. spheres with constant temperature and spheres with uniform temperature. The values of the *Nu* numbers during the interaction depend on the values of the spheres temperature and temperature gradients in the vicinity of the surfaces of the spheres. For the spheres with uniform temperature, the values of the spheres temperature and temperature gradients depend on volume heat capacity ratio. We can imag-

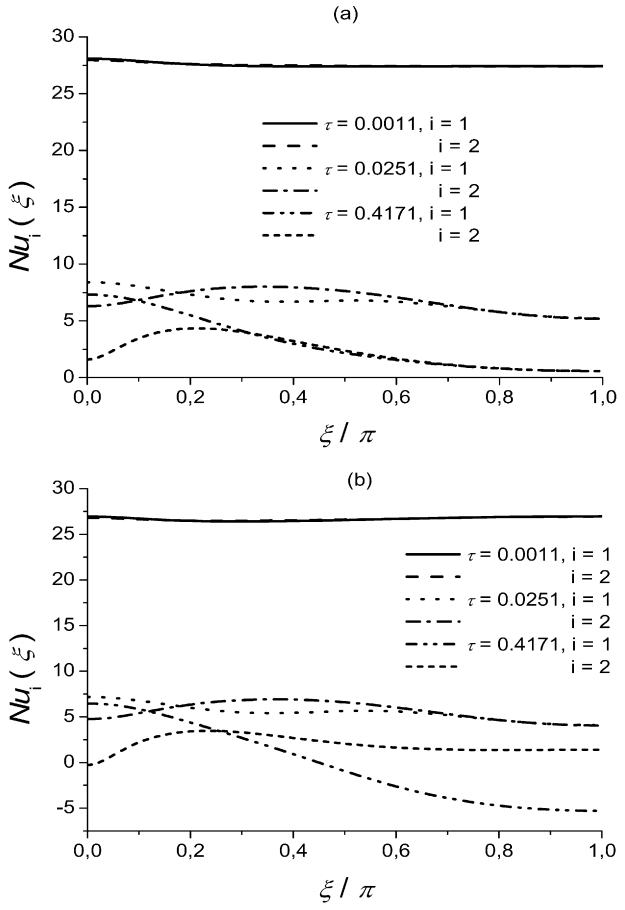

Fig. 6. Local *Nu* numbers at different times for $2L/d = 1.25$; (a) spheres with constant temperature; (b) spheres with uniform temperature.

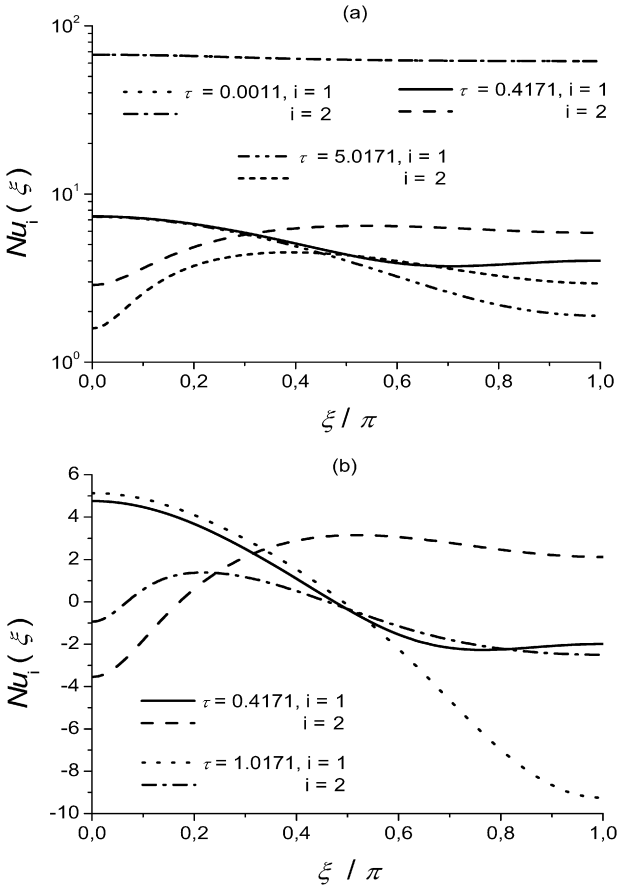

Fig. 7. Local *Nu* numbers at different times for $2L/d = 2$; (a) spheres with constant temperature; (b) spheres with uniform temperature.

ine that Ξ acts as a barrier that controls the heat released in the fluid phase. High values of Ξ means slow release of heat, slow decrease in spheres temperature and high values of the temperature gradients. Small values of Ξ means fast release of heat, fast decrease in spheres temperature and small values for the temperature gradients.

If the interaction takes place at relatively high values of spheres temperature and temperature gradients (for spheres with uniform temperature this condition is satisfied at high values of Ξ and/or small values of $2L/d$) the behaviour of the two systems is similar. Figs. 4(c), 4(d) and 6 show that for $2L/d = 1.25$, in the moment of *Nu* numbers separation, the values of the dimensionless temperature of the spheres and the temperature gradients are comparable. The values of Nu_1 in the separation point are also comparable. At small gaps the interaction occurs and develops in the transition regime. The first stage of interaction does not take too long. Of course, the asymptotic behaviour of the two systems is different. For spheres with uniform temperature at large times, in the convection regime, the temperature of the spheres decreases significantly and thermal wake occurs. The leading sphere exhibits a higher heat transfer rate and its temperature decreases faster. When the difference between the temperatures of the two spheres becomes significant, the impact of the leading sphere decreases and the heat transfer rate of the trailing sphere increases.

For $2L/d = 2$, the interaction occurs in the convection regime. The increase in the distance between spheres increases the duration of the first stage of interaction. In the separation point, the temperature of the spheres is small, the temperature gradients are small and thermal wake is present on both spheres. The capacity of the spheres to transfer heat to the environment is reduced to the area of positive local *Nu* values. For negative local *Nu* values the spheres take heat from the medium. It was expected that the presence of the thermal wake on the leading sphere will decrease the interaction effects. The present results show that the trailing sphere enlarges the thermal wake of the leading sphere and the cooling of the fluid elements in this wake is not strong enough to reduce the interaction effects for the trailing sphere. The result is a global decrease in the heat transfer rate of the system. In the separation point, the value of Nu_1 is smaller than that obtained at $2L/d = 1.25$.

4.2. Spheres with equal diameters and different physical properties

For $\Xi_1 \neq \Xi_2$ and $d_1 = d_2 = d$, the time evolution of the average *Nu* numbers is presented in Figs. 8. In Figs. 8 the case $\Xi_1 = \Xi_2$ is plotted as comparison criterion for the leading sphere. The results presented in Figs. 8 are not the only simulations made with different values of the volume heat capacity

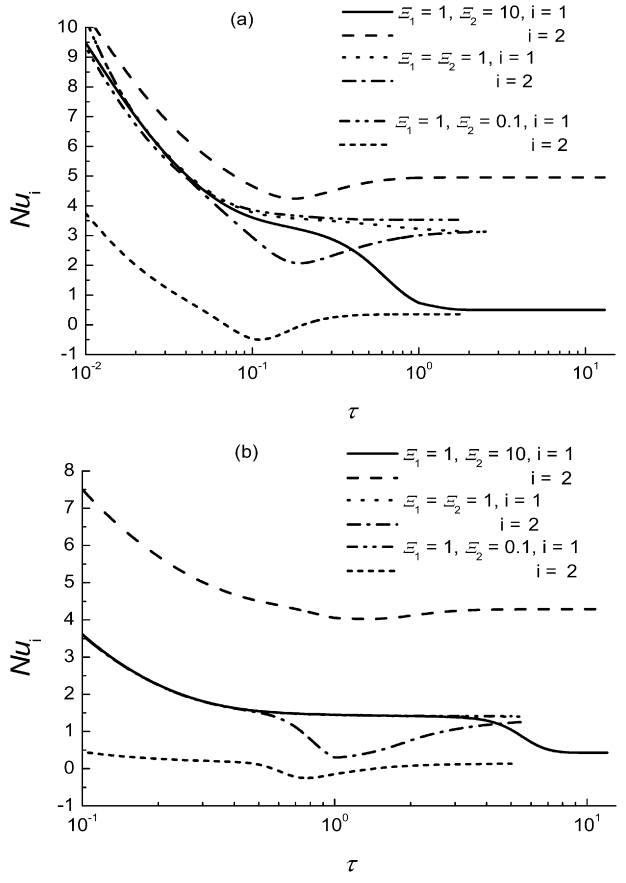

Fig. 8. Time variation of the average *Nu* numbers for $\Xi_1 \neq \Xi_2$; (a) $2L/d = 1.25$; (b) $2L/d = 2$.

ratio. The same behaviour was observed for other (Ξ_1, Ξ_2) values.

Figs. 8 show that:

- for $\Xi_1 > \Xi_2$, the behaviour of the leading sphere during the interaction does not change significantly in comparison with the case $\Xi_1 = \Xi_2$; for $2L/d = 2$, the values of Nu_1 for $\Xi_1 = 1$, $\Xi_2 = 0.1$ and the values of Nu_1 calculated for $\Xi_1 = \Xi_2 = 1$ overlap; for $2L/d = 1.25$, the asymptotic values of Nu_1 are a bit higher; for both $2L/d$ values, Nu_2 exhibits smaller values than those computed for the trailing spheres at $\Xi_1 = \Xi_2 = 0.1$; negative values of Nu_2 occur for $2L/d = 1.25$;
- for $\Xi_1 < \Xi_2$ the trailing sphere exhibits higher *Nu* number values than the leading sphere; for each $2L/d$ value, the asymptotic Nu_2 values computed for $\Xi_1 = 1$ and $\Xi_2 = 10$ are higher than those calculated for $\Xi_1 = \Xi_2 = 10$; for $2L/d = 2$ and $Z_1 \geqslant 10^{-3}$, the values of Nu_1 are approximately equal with those computed for $\Xi_1 = \Xi_2 = 1$ (graphically, these values overlap); the decrease in Nu_1 takes place at very small values of Z_1, i.e. $10^{-4} \leqslant Z_1 \leqslant 10^{-3}$; however, the relevance of this situation for practical situations is questionable; for $2L/d = 1.25$, Nu_1 has smaller values than those computed for $\Xi_1 = \Xi_2 = 1$.

For an isolated sphere, at a given *Pe* number, the parameter that controls the heat transfer is the volume heat capacity ratio. The results presented previously show that, for two spheres of equal diameters in tandem, independent of the sphere's position (upstream or downstream), the volume heat capacity ratio has the same determinant role.

We consider that the general principles of the interaction mechanism presented in the previous section may be used in order to explain the interaction between two spheres in tandem with different Ξ values. Some assumptions as "*both spheres behaves as a single object, with the same average heat transfer rate*" do not remain valid. The separation point is not present. However, we may assume that:

- two stages of interaction exist;
- an analogue of the separation point can be defined;
- depending on the gap between spheres and the values of the volume heat capacity ratio, the interaction takes place at high or small values of the dimensionless temperature of the spheres; also, interaction between spheres with highly different dimensionless temperature can occur in this case.

From the data presented in this section, we think that the case $\Xi_1 < \Xi_2$ deserves some supplementary discussions. Figs. 8 show that the time evolution of Nu_2 has a minimum value. The analogue of the separation point is placed before the minimum value of Nu_2. In the time interval,—analogue of the separation point, minimum Nu_2 value—the leading sphere exerts its maximum pressure on the trailing sphere. Favored by convection, it tries to take the control of the process. This action fails due to the fact that $\Xi_1 < \Xi_2$. If $\Xi_1 < \Xi_2$, Z_1 decreases considerably faster than Z_2.

4.3. Spheres with different diameters

The cases considered of interest and presented in this section are:

(i) $\Xi_1 = \Xi_2$ and $d_1/d_2 = 2$;
(ii) $\Xi_1 = \Xi_2$ and $d_1/d_2 = 0.5$;
(iii) $\Xi_1 < \Xi_2$ and $d_1/d_2 = 2$;

For cases (i) and (ii) we considered only one value for $2L_1/d_1$, i.e. $2L_1/d_1 = 1.25$. In these situations the increase in $2L_1/d_1$ decreases the asymptotic *Nu* values and does not exhibit any other particular effect. For the case (iii), two values of $2L_1/d_1$ were considered: $2L_1/d_1 = 1.25$ and $2L_1/d_1 = 2$.

Fig. 9(a) shows that for $\Xi_1 = \Xi_2$ and $d_1/d_2 = 2$, the dominant role of the leading sphere increases. In comparison with the case $\Xi_1 = \Xi_2$ and $d_1 = d_2$, Nu_1 has higher asymptotic values while Nu_2 has smaller asymptotic values. In case (ii), Nu_2 exhibits greater asymptotic values than Nu_1 (see Fig. 9(b)). The significant decrease in Nu_1 at large times (Fig. 9(b)) is less important. It takes place at very small values of Z_1.

Fig. 10 shows that:

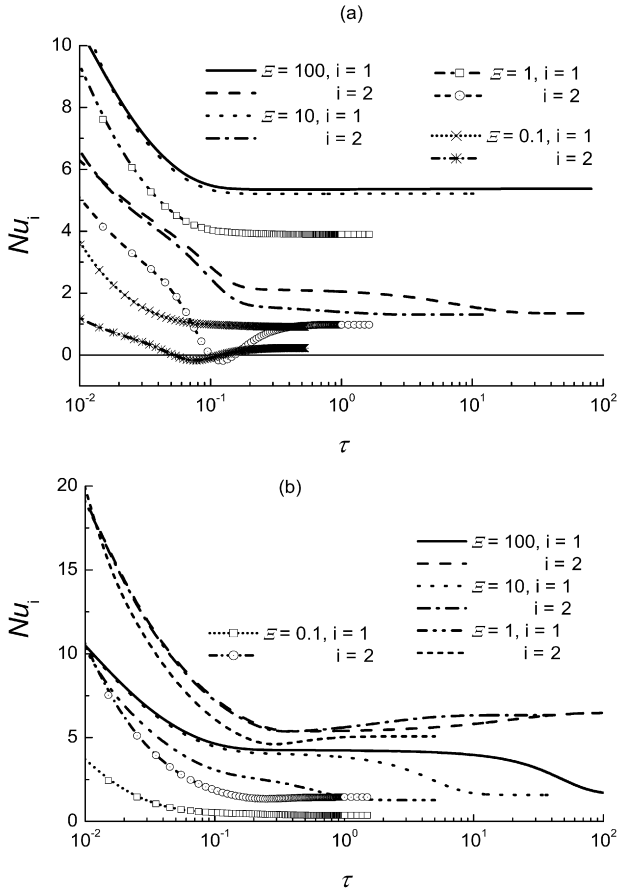

Fig. 9. Time variation of the average *Nu* numbers for spheres with different diameters, $\Xi_1 = \Xi_2$ and $2L_1/d_1 = 1.25$; (a) $d_1/d_2 = 2$; (b) $d_1/d_2 = 0.5$.

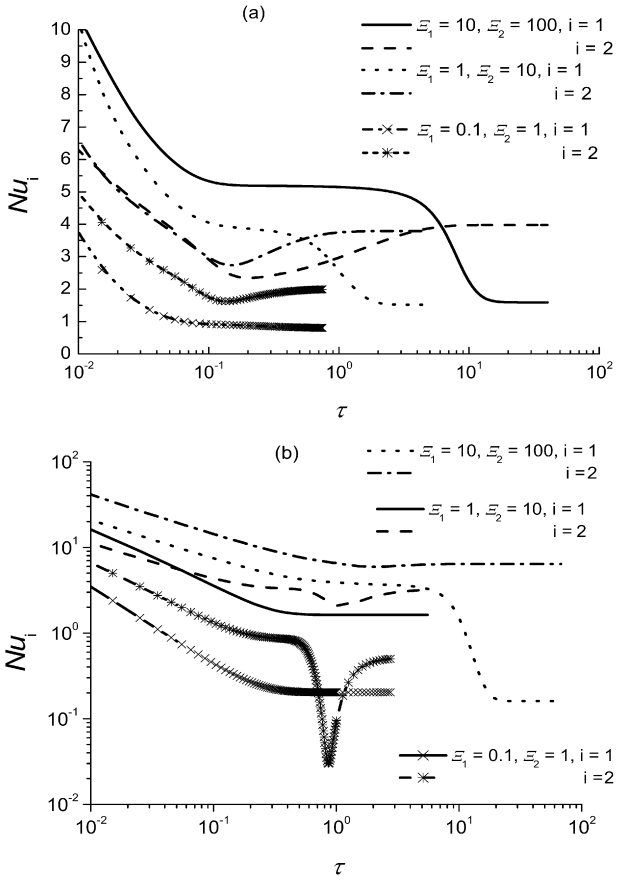

Fig. 10. Time variation of the average *Nu* numbers for spheres with different diameters, $\Xi_1 < \Xi_2$ and $d_1/d_2 = 2$; (a) $2L_1/d_1 = 1.25$; (b) $2L_1/d_1 = 2$.

- at small gaps and high values of volume heat capacity ratio ($\Xi_2 > \Xi_1 \geqslant 1$), as long as Z_1 does not take very small values, the convection effects counterbalance the influence of Ξ; the average *Nu* number of the leading sphere is greater than the average *Nu* number of the trailing sphere;
- in the other situations, i.e. $2L_1/d_1 = 1.25$ and $\Xi_i \leqslant 1$ and the data presented in Fig. 10(b), the volume heat capacity ratio makes the interaction rules; Nu_2 has greater asymptotic values than Nu_1.

We think that supplementary discussions are not necessary in this section. The cases (i)–(iii) can be explained by the arguments presented in the previous sections.

5. Conclusions

This work investigated numerically the thermal interaction between two spheres with spatially uniform temperature in tandem at moderate values of the *Pe* number. Stokes flow around the spheres was assumed. Three cases were considered: (a) equal spheres with identical physical properties; (b) equal spheres with different physical properties and (c) spheres of different sizes with identical/different physical properties.

The present numerical results show that the classical rules of tandem interaction, rules established for spheres with constant temperature, are not obeyed by the spheres with spatially uniform temperature but variable in time. For equal spheres with identical physical properties the most relevant aspects are: (a) in almost all situations the increase in the distance between spheres does not increase the asymptotic *Nu* values; (b) Nu_1 and Nu_2 tend to the same asymptotic value.

A mechanism that explains this behaviour is presented. The key parameters that control the process are: the gap between spheres and the volume heat capacity ratio. Small gaps and high values of the volume heat capacity ratio lead to high asymptotic *Nu* values. For spheres of different sizes and/or different materials, the convection cannot counteract in any situation the effect of geometry and/or the effect of volume heat capacity ratio. In these situations, the trailing sphere may exhibit higher *Nu* values than the leading sphere.

References

[1] R. Clift, J.R. Grace, M.E. Weber, Bubbles, Drops and Particles, Academic Press, New York, 1978.
[2] H. Brauer, Unsteady state mass transfer through the interface of spherical particles −I + II, Int. J. Heat Mass Transfer 21 (1978) 445–465.
[3] B.I. Brounshtein, V.V. Shegolev, Hydrodynamics, Mass and Heat Transfer in Column Devices, Khimiya, Leningrad, 1988 (in Russian).
[4] S.S. Sadhal, P.S. Ayyaswamy, J.N.-C. Chung, Transport Phenomena with Drops and Bubbles, Springer, Berlin, 1996.
[5] R.P. Chhabra, Bubbles, Drops, and Particles in Non-Newtonian Fluids, CRC Press, Boca Raton, 2006.

[6] E.E. Michaelides, Particles, Bubbles and Drops—Their Motion, Heat and Mass Transfer, World Scientific, Singapore, 2006.
[7] A.R.H. Cornish, Note on minimum possible rate of heat transfer from a sphere when other spheres are adjacent to it, Trans. Instn. Chem. Engrs. 43 (1965) 332–333.
[8] E.M. Twardus, T.A. Brzustowski, The interaction between two burning fuel droplets, in: 5th Int. Symp. on Combustion Processes, Krakow, Poland, September 1972 (as cited in [11]).
[9] M. Labowsky, Calculation of the burning rates of interacting fuel droplets, Combust. Sci. Technol. 22 (1980) 217–220.
[10] A. Umemura, S. Ogawa, N. Oshima, Analysis of the interaction between two burning droplets, Combust. Flame 41 (1981) 35–44.
[11] A. Umemura, S. Ogawa, N. Oshima, Analysis of the interaction between two burning fuel droplets of different sizes, Combust. Flame 41 (1981) 111–191.
[12] K. Aminzadeh, T.R. al Taha, A.R.H. Cornish, M.S. Kolansky, R. Pfeffer, Mass transport around two spheres at low Reynolds numbers, Int. J. Heat Mass Transfer 17 (1974) 1425–1436.
[13] R. Tal (Thau), D.N. Lee, W.A. Sirignano, Heat and momentum transfer around a pair of spheres in viscous flow, Int. J. Heat Mass Transfer 27 (1984) 1953–1962.
[14] C.-K. Chen, K.-L. Wong, S.-C. Lee, The finite element solution of laminar combined convection from two spheres in tandem arrangement, Computer Meth. Appl. Mechanics & Engrg. 59 (1986) 73–84.
[15] O.M. Lavrenteva, A.M. Leshansky, A. Nir, Spontaneous thermocapillary interaction of drops, bubbles and particles: Unsteady convective effects at low Peclet numbers, Phys. Fluids 11 (1999) 1768–1780.
[16] R. Balasubramanian, R.S. Subramanian, Axisymmetric thermal wake interaction of two bubbles in a uniform temperature gradient at large Reynolds and Marangoni numbers, Phys. Fluids 11 (1999) 2856–2864.
[17] O.M. Lavrenteva, A. Nir, Spontaneous thermocapillary interaction of drops: Unsteady convective effects at high Peclet numbers, Phys. Fluids 13 (2001) 368–381.
[18] A.M. Leshansky, O.M. Lavrenteva, A. Nir, Thermocapillary migration of bubbles: Convective effects at low Peclet number, J. Fluid Mech. 443 (2001) 377–401.
[19] R.S. Ramachandran, C. Kleinstreuer, T.-W. Wang, Forced convection heat transfer of interacting spheres, Numer. Heat Transfer A 15 (1989) 471–487.
[20] A. Maheshwari, R.P. Chhabra, G. Biswas, Effect of blockage on drag and heat transfer from a single sphere and an in-line array of three spheres, Powder Technology 168 (2006) 74–83.
[21] P.M. Morse, H. Feshbach, Method of Theoretical Physics, II, McGraw-Hill, New York, 1953.
[22] J. Happel, H. Brenner, Low Reynolds Number Hydrodynamics, Nijhoff, Hague, 1984.
[23] E.W. Weisstein, Bispherical coordinates, MathWorld—A Wolfram web resource, http://mathworld.wolfram.com/BisphericalCoordinates.html.
[24] Gh. Juncu, Numerical study of axisymmetric slow viscous flow past two spheres, in: Mathematical Modelling of Environmental and Life Sciences Problems, Proc. 4th Workshop September 2005 Constanta, Academiei, Bucharest, 2006, pp. 109–117.
[25] P.W. Hemker, A numerical study of stiff two-point boundary problems, PhD thesis, Mathematisch Centrum, Amsterdam, 1977.
[26] M. Stimson, G.B. Jeffery, The motion of two spheres in a viscous fluid, Proc. R. Soc. A 11 (1926) 110–116.